www.czasopisma.pan.pl PAN POLSKA AKADEMIA NAUK www.journals.pan.pl

Arch. Metall. Mater. **63** (2018), 3, 1401-1409

DOI: 10.24425/123818

D. BOCHENEK*#, K. OSIŃSKA*, P. NIEMIEC*, M. ADAMCZYK*,
T. GORYCZKA**, R. SZYCH*

TECHNOLOGY AND ELECTROPHYSICAL PROPERTIES OF THE $(K_{0.44}Na_{0.52}Li_{0.04})NbO_3$ CERAMICS DOPED BY Cr^{3+}, Zn^{2+}, Sb^{3+} OR Fe^{3+}

In the work five ceramic compounds based on the $(K_{0.44}Na_{0.52}Li_{0.04})NbO_3$ (KNLN) material modified with oxides: Cr_2O_3, ZnO, Sb_2O_3 or Fe_2O_3 (in an amount of 0.5 mol.%) were obtained. The KNLN-type composition powder was prepared by solid phase synthesis from a mixture of simple oxides and carbonates, while compacted of the ceramic samples was conducted by free sintering methods. In the work the effect of the used admixture on the electrophysical properties of the KNLN ceramics was presented. The XRD, EDS tests, the SEM measurements of the morphology ceramic samples, dielectric properties and DC electric conductivity were conducted.

The research showed that the used admixtures introduced into the base of KNLN-type composition improve the microstructure of the ceramic samples and improve their sinterability. In the case of the dielectric measurements, it was observed a decrease in the maximum dielectric permittivity at the T_C for dopred KNLN-type samples. The addition of an admixture of chromium, zinc, antimony or iron in an amount of 0.5 mol.% to the base composition $(K_{0.44}Na_{0.52}Li_{0.04})NbO_3$ practically does not change the phase transition temperature. The diminution in the density value of doped KNLN ceramics was attributed to the alkali elements volatilization.

Keywords: lead free ceramics, KNLN ceramics, SEM microstructure, dielectric tests

1. Introduction

The main basis for obtaining functional ceramic materials and used extensively in modern microelectronics is a multicomponent solid solution based on the $PbZr_{1-x}Ti_xO_3$ [1-4]. Since the main drawback of PZT is the presence of lead in its composition, other lead-free materials that can replace the PZT in selected applications are sought for [5-7]. One of the candidates for such possibilities, with good electrophysical properties, is sodium potassium niobate $(K,Na)NbO_3$ (KNN) [8-9]. KNN material is subjected to various modifications [10-15]. KNN have a perovskite structure of the general formula ABO_3, where the potassium K^+ cation and sodium Na^+ cation are substituted for position A, while the niobium Nb^{5+} cation is located in position B elementary cell [16]. At room temperature, the KNN ceramics are crystallized in the orthorhombic system in the A*mm2* symmetry. Above room temperature in KNN there are two phase transitions: at low temperature and at high temperature. The low-temperature phase transition from the orthorhombic phase to the tetragonal phase occurs below 200°C, whereas the high-temperature phase transition from the tetragonal ferroelectric phase to the paraelectric (regular) phase occurs close to 400°C [17].

The purpose of the work was obtaining the five ceramic compounds based on the doped sodium potassium niobate $(K_{0.44}Na_{0.52}Li_{0.04})NbO_3$ (KNLN) modified with oxides: Cr_2O_3, ZnO, Sb_2O_3 or Fe_2O_3 (in an amount of 0.5 mol.%) and investigating the effect of the used admixture on the electrophysical properties of KNLN ceramics. In the process of obtaining ceramic compositions, molar excess doping was used.

2. Experimental

Five ceramic compositions based on the $(K_{0.44}Na_{0.52}Li_{0.04})NbO_3$ (KNLN) doped with chromium (III) oxide, zinc (II) oxide, antimony (III) oxide or iron (III) oxide were designed and obtained. The KNLN composition powder was prepared by solid phase synthesis from a mixture of simple oxides and carbonates according to the reaction equation:

$$0.22\ K_2CO_3 + 0.26\ Na_2CO_3 + 0.02\ Li_2CO_3 + \\ + 0.5\ Nb_2O_5 \rightarrow (K_{0.44}Na_{0.52}Li_{0.04})NbO_3 + 0.5\ CO_2\uparrow.$$

Before the synthesis of the $(K_{0.44}Na_{0.52}Li_{0.04})NbO_3$ (KNLN) composition, appropriate metal oxides were added to

* UNIVERSITY OF SILESIA IN KATOWICE, FACULTY OF COMPUTER SCIENCE AND MATERIAL SCIENCE, INSTITUTE OF TECHNOLOGY AND MECHATRONICS 12, ŻYTNIA ST., 41-200, SOSNOWIEC, POLAND
** UNIVERSITY OF SILESIA IN KATOWICE, FACULTY OF COMPUTER SCIENCE AND MATERIAL SCIENCE, INSTITUTE OF MATERIAL SCIENCE, 1A, 75 PUŁKU PIECHOTY ST., 41-500 CHORZÓW, POLAND
# Corresponding author: dariusz.bochenek@us.edu.pl

obtain the following chemical compositions: $(K_{0.44}Na_{0.52}Li_{0.04})NbO_3$ + 0.5%mol.Cr_2O_3 (KNLNCr), $(K_{0.44}Na_{0.52}Li_{0.04})NbO_3$ + 0.5%mol.ZnO (KNLNZn), $(K_{0.44}Na_{0.52}Li_{0.04})NbO_3$ + 0.5%mol. Sb_2O_3 (KNLNSb), $(K_{0.44}Na_{0.52}Li_{0.04})NbO_3$ + 0.5%mol.Fe_2O_3 (KNLNFe). As substrates for the synthesis, potassium carbonate K_2CO_3, (POCH, 99.99%), sodium carbonate Na_2CO_3 (SIGMA-ALDRICH, 99.5%), lithium carbonate Li_2CO_3 (SIGMA-ALDRICH, 99%), niobium oxide Nb_2O_5 (SIGMA-ALDRICH, 99.9%) were used as well as chromium (III) oxide Cr_2O_3 (POCH, 99.9%), zinc (II) oxide ZnO (POCH, 99.99%), antimony (III) oxide Sb_2O_3 (ALDRICH, 99%), iron (III) oxide Fe_2O_3 (CHEMPUR, 99.9%). The reaction substrates, weighed in stoichiometric amounts, were wet mixed in ethanol (POCH, 99.99%), in a planetary mill for 24 h. After drying, the ceramic powder of each composition was pressed into pallets and the synthesis was carried out at following condition 900°C/4 h. After the synthesis, the samples were cleaned, and grounded again in a planetary mill (24 h). Next, the powders were formed into discs with diameter d = 10 mm and then compacted by free sintering methods at following condition 1110°C/ 2 h (the rate of temperature increase in a furnace was 5°C/min.). After sintering, the ceramic samples were subjected to grinding, polishing and annealing (to remove mechanical stresses), and then silver electrodes were applied to their surfaces.

The apparent density of the sintered samples was measured by the Archimedes method. X-ray diffraction patterns (XRD) of the KNLN-type samples were measured using X'Pert-Pro PW3040/60 diffractometer ($\lambda Cu_{K\alpha 1}$ = 1.54056 Å). All X-ray diffraction patterns were registered at room temperature, in 2θ range: 10 to 130º in steps-scan mode: 0.05° and 4 s/step. The SEM morphology of the ceramic samples was observed by scanning electron microscopy JSM-7100F TTL LV Field Emission Scanning Electron Microscope. The stoichiometry of the ceramic samples was studied with the EDS chemical composition analysis system. Dielectric properties (dielectric permittivity and dielectric loss) were measured by QuadTech 1920 Precision LCR meter in the temperature range of 20°C to 550°C in the frequency range from 1 kHz to 100 kHz. Measurements of DC electric conductivity were performed using a 6517B Keithley electrometer in the temperature range from 20°C to 520°C.

3. Results and discussion

As the technological process was carried out in the same conditions, it allowed comparing the effect of the introduced admixture on the electrophysical properties of the KNLN-type materials. Fig. 1 shows the relative density *RD* of the doped KNLN-type ceramics obtained in the same technological conditions. Doping the basic composition of KNLN with chromium, zinc, antimony or iron reduces the density of ceramic samples. The highest apparent density values for doped compositions (Table 1) are observed for the KNLNSb samples (with antimony) while the smallest is for the KNLNFe samples (with an iron). Ions of the Cr^{3+}, Sb^{3+}, Zn^{2+}, Fe^{3+} replace alkaline elements in A-positions of the KNLN perovskite lattice. The incorporation of these additions at the initial stage of the $(K_{0.44}Na_{0.52}Li_{0.04})NbO_3$ synthesis, can increase the A-site replacement what contributes to the loss of the alkali elements (mainly sodium). The diminution in the density value of doped samples was attributed to the alkali elements volatilization.

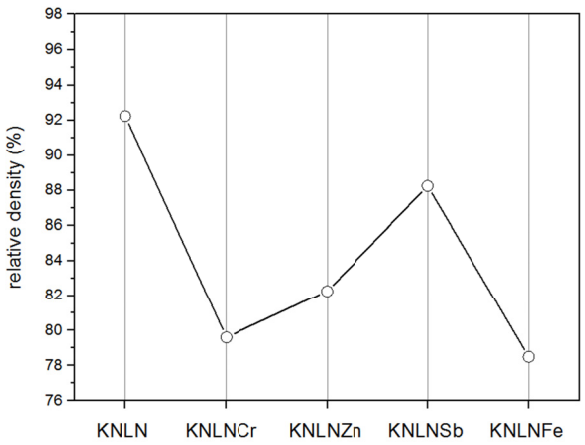

Fig. 1. The relative density *RD* of the KNLN-type ceramics

TABLE 1

Electrophysical properties of the KNLN-type ceramics

	KNLN	KNLNCr	KNLNZn	KNLNSb	KNLNFe
ρ (g/cm^3)	4.16	3.59	3.71	3.98	3.54
RD (%) [a]	92.24	79.60	82.26	88.25	78.49
ε' at T_r [b]	397	268	360	448	310
tanδ at T_r [b]	0.034	0.099	0.122	0.121	0.067
$T_{O\text{-}T}$ (°C) [b]	138	166	160	150	161
ε' at $T_{R\text{-}T}$ [b]	795	607	713	800	697
T_C (°C) [b]	418	420	418	418	418
ε' at T_C [b]	4972	3785	4437	4744	3567
tanδ at T_C [b]	0.105	0.221	0.286	0.096	0.217
ρ_{DC} at T_r (Ωm)	$4.701\cdot10^6$	$4.305\cdot10^6$	$4.011\cdot10^7$	$2.256\cdot10^7$	$6.104\cdot10^5$

[a] – theoretical density of undoped KNN ceramics is 4.51 g/cm [22],
[b] – data for 10 kHz,
T_r – room temperature.

Fig. 2 presents the results of XRD tests of the KNLN-type ceramics measured at room temperature. In order to determine lattice parameter, the X-ray diffraction pattern was fitted using the Rietveld method [18-19]. The analysis showed that all obtained KNLN-type ceramic samples have a two-phase perovskite structure with orthorhombic and tetragonal systems (Table 2). The symmetry of crystal lattice of the tetragonal perovskite (a small percentage share) was described with space group P*4bm,* whereas symmetry of the orthorhombic one (with a dominant percentage) was described by A*mm2*.

Fig. 3 shows the SEM morphology of the fracture of the KNLN-type ceramic samples. The microstructural images for each KNLN-type ceramics show a significant porosity. The microstructure of undoped KNLN ceramics is characterized by a fine grain, with a characteristic cube shape – average grain size

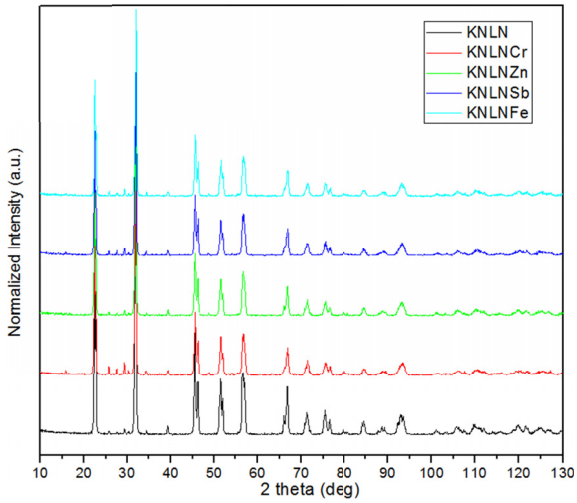

Fig. 2. The XRD patterns of the KNLN-type ceramics

TABLE 2

Lattice parameters of the KNLN-type calculated by the Rietveld method.

Sample	Crystallographic system	Lattice parameters			
		a_0 (Å)	b_0 (Å)	c_o (Å)	V_o (Å^3)
KNLN	orthorhombic	3.9401	5.6315	5.6633	125.6611
	tetragonal	12.5962	12.5962	3.9364	624.5659
KNLNCr	orthorhombic	3.9439	5.6258	5.6604	125.5906
	tetragonal	12.5737	12.5737	3.9373	622.4789
KNLNZn	orthorhombic	3.9451	5.6319	5.6651	125.8695
	tetragonal	12.5952	12.5952	3.9432	625.5456
KNLNSb	orthorhombic	3.9455	5.6312	5.6640	125.8422
	tetragonal	12.6085	12.6085	3.9429	626.8197
KNLNFe	orthorhombic	3.9471	5.6355	5.6639	125.9871
	tetragonal	12.5882	12.5882	3.9422	624.6919

is 3.68 μm (Fig. 3a). The morphology of the KNLN ceramics has a high degree of sintering, in which the breakthrough occurs through grain (breaking of intra-granular). This proves greater mechanical strength of the grain boundaries, at the expense of the grain's interior strength.

Introduced admixtures into the base KNLN composition improve the microstructure of the ceramic samples and improve their sinterability. The admixture of Cr^{3+} introduced into the basic composition of KNLN causes the most changes in the microstructure of ceramics (Fig. 3b). The addition of chromium significantly

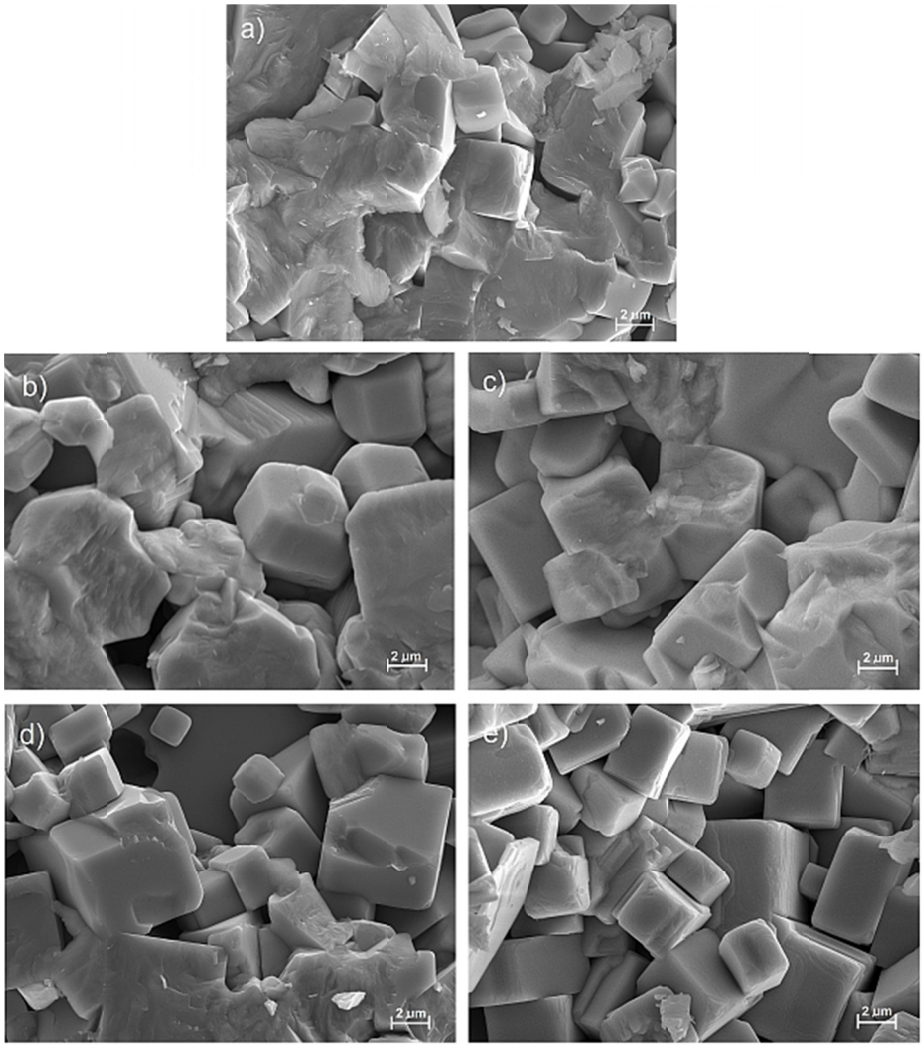

Fig. 3. SEM micrographs of the KNLN-type ceramics: KNLN (a), KNLNCr (b), KNLNZn (c), KNLNSb (d), KNLNFe (e)

increases the average grain size (5.32 μm), causing at the same time a change in the shape of grains from a cubic shape (with a square cross-section) to grains with a cross-section of polyhedrons. For the KNLNCr sample, there is a cracking mechanism that occurs both on the grain boundary and through grain.

The admixture of Zn also causes increase in the average grain size of KNLNZn ceramics (5.79 μm), and the nature of cracks in the microstructure indicates a higher proportion of intra-grain cracking (higher strength of grain boundaries, at the expense of grain interior) – Fig. 3c. The admixture of antimony, Sb^{3+} increases the average grain size of the microstructure (3.97 μm), causing deformation of the cubic shapes of KNLNSb ceramic grains (Fig. 3d). At the same time, the degree of inhomogeneity of the microstructure increases (there are both small grains and large-sized grains). It is related to the uneven growth of grains in the entire volume of the sample (large grains grow faster at the expense of small grains). For this sample, the microstructure has a two-element fracture mechanism: the cracking at the grain boundary and the intra-grain cracking. The admixture of iron, Fe^{3+} slightly increases the heterogeneity of the microstructure (Fig. 3e) and decreases the average grain size of the KNLNFe ceramics (3.26 μm), which retain the shape of the regular cubes. Fe^{3+} introduced to KNLN composition additionally increases the grain's internal strength (the fracture occurring on the grain border is the dominant mechanism). Similar microstructural images for KNN ceramics doped with Li and Sb were presented by Rani et al. [20] and Qian et.al. [21].

The obtained material was subjected to tests of composition homogeneity by EDS analysis (Fig. 4). Theoretical and experimental percentages of elements (expressed as oxides) of ceramic samples are given in the Table 3. The EDS analysis of the element distribution confirmed the qualitative chemical composition of doped $(K_{0.44}Na_{0.52}Li_{0.04})NbO_3$ ceramics. Compared to theoretical calculations sodium and potassium deficiency and a small excess of niobium are observed for all obtained compositions. All deviations from the initial composition are within the acceptable range.

Fig. 5 shows the temperature dependence of the dielectric permittivity of the obtained KNLN-type compositions, measured at frequencies from 1 kHz to 100 kHz. In the $\varepsilon(T)$ plots there

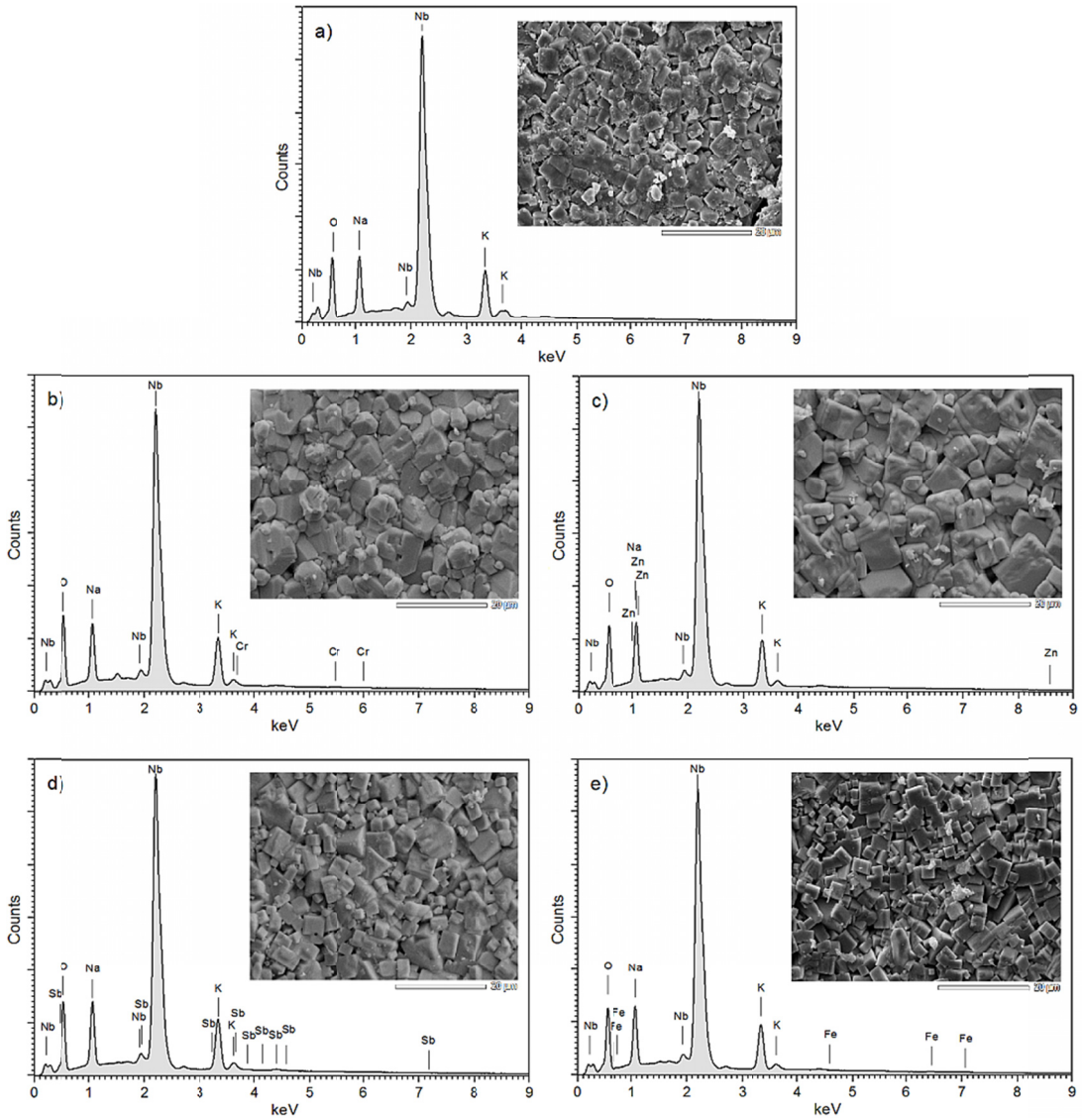

Fig. 4. EDS analysis of the element distribution of the KNLN-type ceramics: KNLN (a), KNLNCr (b), KNLNZn (c), KNLNSb (d), KNLNFe (e)

TABLE 3

Theoretical and experimental percentages of elements of the KNLN-type ceramics

Oxide formula	Composition									
	KNLN		KNLNCr		KNLNZn		KNLNSb		KNLNFe	
	Theoret. (%)	Exper. (%)	Theoret. (%)	Exper. (%)	Theoret. (%)	Exper. (%)	Theoret. (%)	Exper. (%)	Theoret. (%)	Exper. (%)
K_2O	12.17	10.35	12.11	10.12	12.14	10.05	12.06	10.98	12.11	9.94
Na_2O	9.46	8.37	9.42	7.96	9.44	8.60	9.38	8.91	9.42	8.80
Li_2O	0.35	—	0.35	—	0.35	—	0.35	—	0.35	—
Nb_2O_5	78.02	81.28	77.68	81.89	77.83	81.15	77.37	79.08	77.66	80.84
Cr_2O_3	—	—	0.44	0.02	—	—	—	—	—	—
ZnO_2	—	—	—	—	0.24	0.20	—	—	—	—
Sb_2O_5	—	—	—	—	—	—	0.85	1.03	—	—
Fe_2O_3	—		—	—	—	—	—	—	0.47	0.42

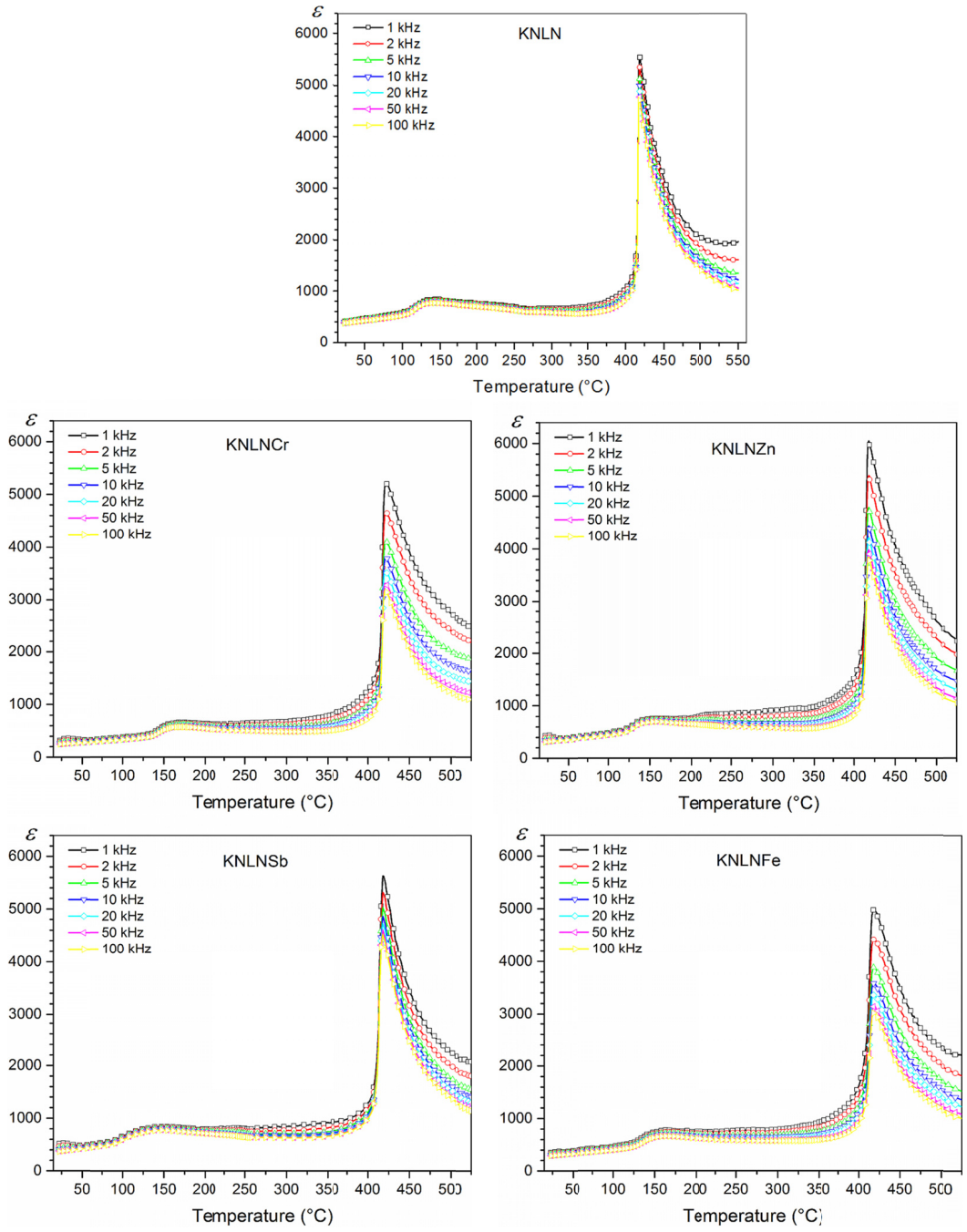

Fig. 5. Temperature dependence of dielectric permittivity of the KNLN-type ceramics for different frequencies of measuring field

are two characteristic maxima. The first local (broad) maximum of dielectric permittivity is associated with antiferroelectric-ferroelectric (orthorhombic-tetragonal) structural transition. The second one, with a sharp of dielectric permittivity (at higher temperature) is connected with the ferroelectric-paraelectric (tetragonal-cubic) phase transition.

The introduction of the admixture (chromium, zinc, antimony or iron) in the amount of 0.5 mol.%, to the basic composition $(K_{0.44}Na_{0.52}Li_{0.04})NbO_3$ practically does not cause the shift of the phase transition temperature (Fig. 6, Table 1). Such doping, however, induces a decrease in the maximum of the dielectric permittivity at the T_C temperature. On the temperature dependences $\varepsilon(T)$, the local broad maximum, does not occur in the same temperature for all doped compositions (Table 1). Similar results of temperature measurements of dielectric permitivitty for Sb and Ta-doped KLNN ceramics were presented by Qian et al. [21].

Fig. 7 shows the frequency dependence of the real dielectric permittivity, ε' of the KNLN-type samples, measured at four temperatures (25°C, 150°C, 300°C and 450°C). The figures

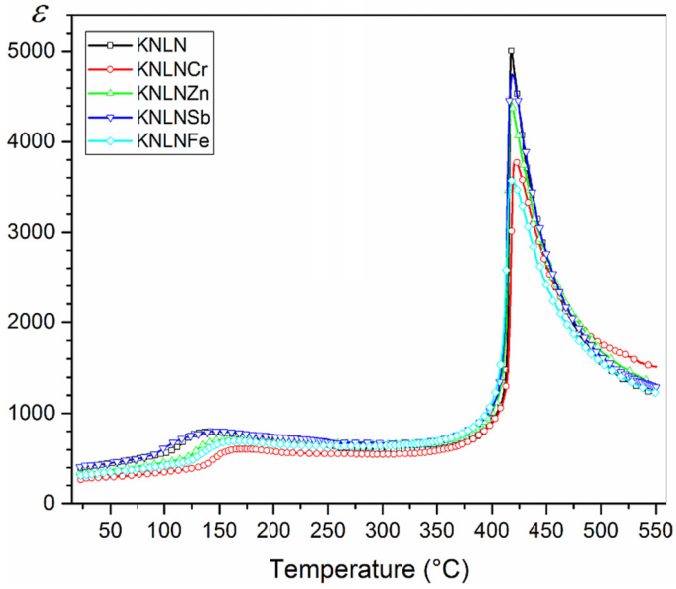

Fig. 6. Temperature dependence of dielectric permittivity of the KNLN-type ceramics for 10 kHz

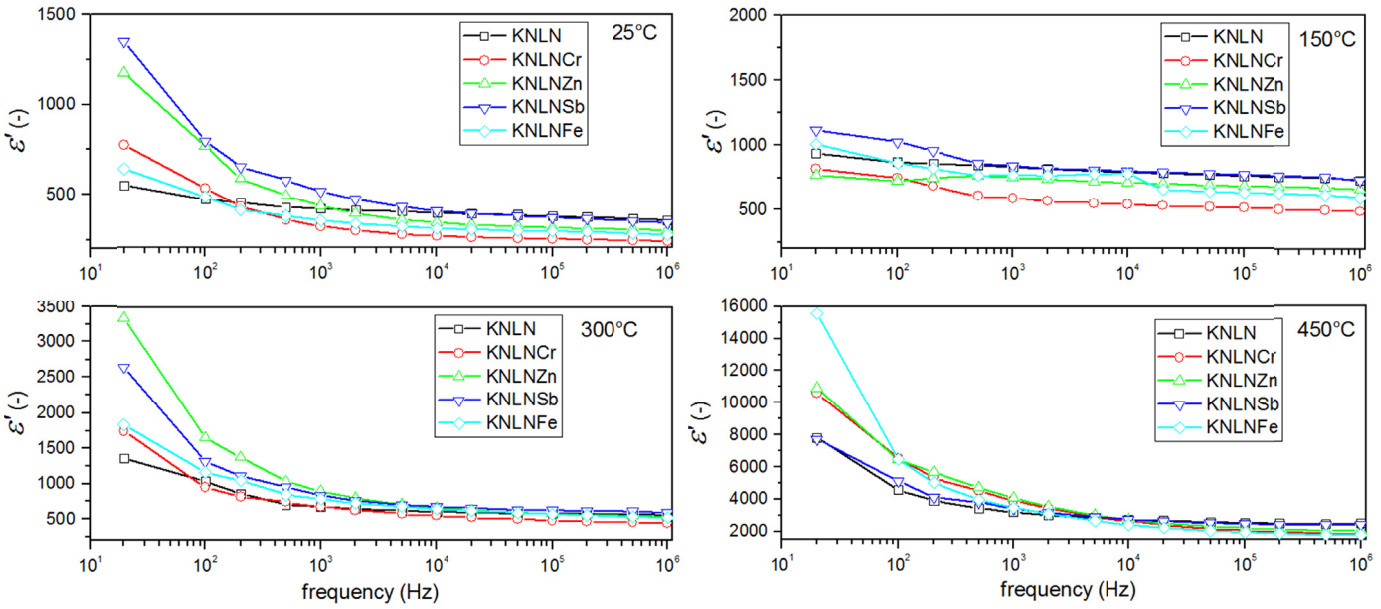

Fig. 7. Frequency dependence of dielectric permittivity for KNLN-type samples at different temperatures

show that all ceramic samples has a similar dielectric behavior depending on the frequency of the measuring field. The KNLN-type samples have a Debye-like relaxation behaviour and the $\varepsilon'(f)$ plots displays a smooth decrease at the frequency.

Fig. 8 shows the temperature dependence of the $\tan\delta$ for the obtained KNLN-type ceramics, measured at frequencies from 1 kHz to 100 kHz. The introduction of the admixture (chromium, zinc, antimony or iron) to the basic composition $(K_{0.44}Na_{0.52}Li_{0.04})NbO_3$, causes an increase in dielectric loss. For all doped compositions up to a temperature of approx. 200°C, the increase in dielectric loss is insignificant (Fig. 9). In the case of the KNLNSb, KNLNFe and KNLNCr samples, in the entire measurement area, the values of the dielecric loss increase not much, while in the case of the KNLNZn sample, in the temperature range from 200°C to 410°C an increase of the dielectric loss is observed.

In the $\ln\sigma_{DC}(1000/T)$ plots, anomalies (changes in the nature of electrical conductivity) are observed for all KNLN-type compositions in the area of phase transitions (Fig. 10). The first one is associated with antiferroelectric-ferroelectric (orthorhombic-tetragonal) structural transition and second one is associated with the ferroelectric-paraelectric (tetragonal-cubic) phase transition. In these areas there is a change in the nature of the electrical conductivity (areas with a negative temperature coefficient of resistance NTCR and a positive temperature coefficient of resistance PTCR). During heating the samples from room temperature, an area with PTCR is observed on the $\ln\sigma_{DC}(1000/T)$ plots. Above the orthorhombic-tetragonal structural transition there

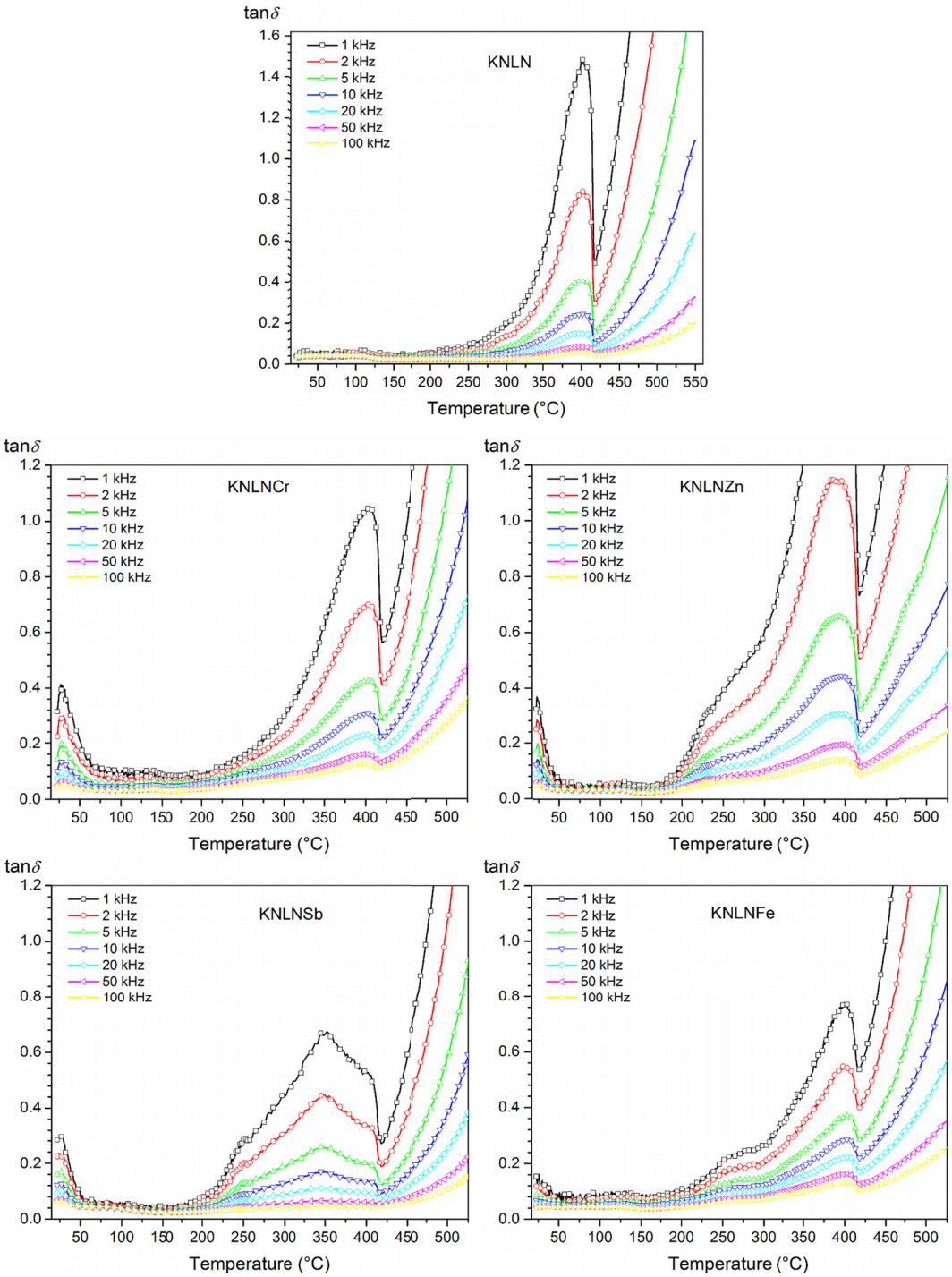

Fig. 8. Temperature dependence of dielectric loss of the KNLN-type ceramics for different frequencies of measuring field

is a smooth change in the nature of the conductivity (the area of NTCR – the electric conductivity increases with temperature). Another change in the nature of electrical conductivity takes place around 100°C before the ferroelectric-paraelectric phase change, where there is a local increase in resistance (the area of PTCR – decrease in the electrical conductivity). In this area, the increase in resistance is not as large as in the previous case. Above the phase transition temperature, a rapid increase in the electrical conductivity (the area of NTCR) is observed, which is also confirmed by the temperature dielectric loss tests of the KNLN-type ceramics.

4. Conclusion

In the work, successfully, five ceramic compounds based on the doped sodium potassium niobate $(K_{0.44}Na_{0.52}Li_{0.04})NbO_3$ (KNLN) modified with oxides: Cr_2O_3, ZnO, Sb_2O_3 or Fe_2O_3 (in an amount of 0.5 mol.%) were obtained. The effect of the admixture used on the electrophysical properties of KNLN ceramics was investigated.

Two maxima are observed on the temperature measurements of dielectric permitivitty. The first one (with broad – local maximum) is associated with antiferroelectric-ferroelectric

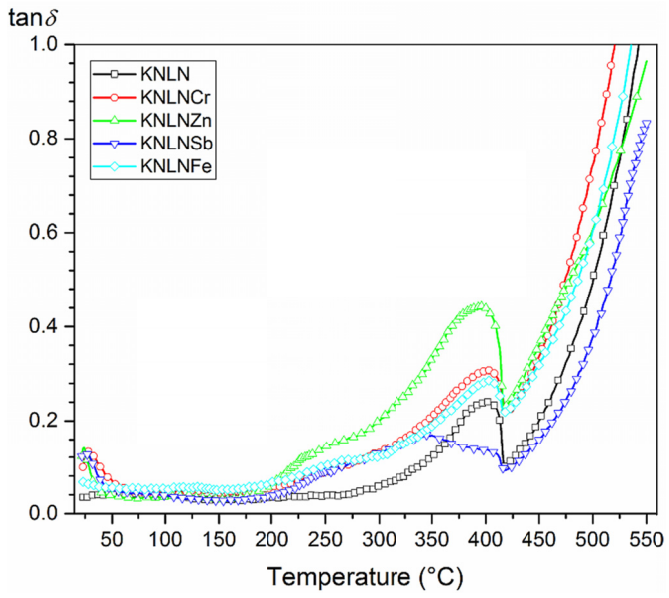

Fig. 9. Temperature dependence of dielectric loss of the KNLN-type ceramics for 10 kHz

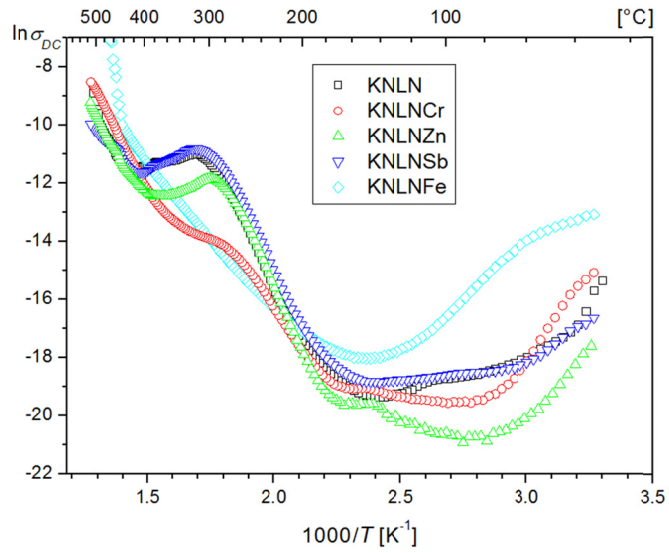

Fig. 10. The $\ln\sigma_{DC}(1000/T)$ graph of the KNLN-type ceramics

(orthorhombic-tetragonal) structural transition, and second one is associated with the ferroelectric-paraelectric (tetragonal-cubic) phase transition. The admixtures introduced into the KNLN causes decrease in the maximum dielectric permittivity at the T_C. The addition of an admixture of chromium, zinc, antimony or iron in an amount of 0.5 mol.% to the base composition $(K_{0.44}Na_{0.52}Li_{0.04})NbO_3$ practically does not change the phase transition temperature.

Considering that Cr^{3+}, Sb^{3+}, Zn^{2+}, Fe^{3+} ions replace alkaline elements in A-positions of the KNLN perovskite lattice, the incorporation of these additions at the initial stage synthesis can increase the A-site replacement and hence the loss of the alkali elements (mainly sodium). The diminution in the density value of doped ceramic was attributed to the alkali elements volatilization.

Studies have shown that the used admixtures introduced into the base of KNLN-type composition improve the microstructure of the ceramic samples and improve their sinterability. This is important information and the technological basis for the further design of chemical compositions from the point of view of usable parameters in micromechatronic applications. Striving to reduce the porosity of ceramic samples during the technological process is advisable e.g. by introducing several admixtures in various amounts (which should improve the electrophysical parameters). Research on the KNLN-type material should be continued towards further improvement all electrophysical properties, obtaining multicomponent lead-free materials (multi-element admixture) which in the future will be able to replace PZT-type piezoceramics.

REFERENCES

[1] M. Venkata Ramana, S. Roopas Kiran, N. Ramamanohar Reddy, K.V. Siva Kumar, V.R.K. Murthy, B.S. Murty, Investigation and characterization of $Pb(Zr_{0.52}Ti_{0.48})O_3$ nanocrystalline ferroelectric ceramics: By conventional and microwave sintering methods, Materials Chemistry and Physics **126**, 295-300 (2011).

[2] R. Skulski, D. Bochenek, P. Wawrzała, G. Dercz, D. Brzezińska, Technology and properties of PBZTS ceramics, International Journal of Applied Ceramic Technology **10**, 2, 330-338 (2013).

[3] R. Zachariasz, D. Bochenek, Parameters of ceramics obtained on the base PZT used to build electroacoustic converters, Journal de Physique IV **137**, 189-192 (2006).

[4] R. Zachariasz, D. Bochenek, K. Dziadosz, J. Dudek, J. Ilczuk, Influence of the Nb and Ba dopands on the properties of the PZT type ceramics, Archives of Metallurgy and Materials **56**, 4, 1217-1222 (2011).

[5] G. Vats, R. Vaish, C.R. Bowen, Selection of Ferroelectric Ceramics for Transducers and Electrical Energy Storage Devices, International Journal of Applied Ceramic Technology **12**, S1, E1-E7 (2015).

[6] G. Vats, R. Vaish, Piezoelectric material selection for transducers under fuzzy environment, Journal of Advanced Ceramics **2**, 2, 141-148 (2013).

[7] G. Vats, R. Vaish, Selection of Lead-Free Piezoelectric Ceramics, International Journal of Applied Ceramic Technology **11**, 5, 883-893 (2014).

[8] G. Vats, R. Vaish, Selection of optimal sintering temperature of $K_{0.5}Na_{0.5}NbO_3$ ceramics for electromechanical applications, Journal of Asian Ceramic Societies **2**, 5-10 (2014).

[9] G.Z. Zang, X.J. Yi, J. Du, Z.J. Xu, R.Q. Chu, P. Fu, W. Li, Microstructure and electric properties of $(Na_{0.015-x}K_x)NbO_3$ lead-free piezoceramics, Journal of Materials Science Materials in Electronics **22**, 1282-1285 (2011).

[10] R.-A. Eichel, E. Erünal, P. Jakes, S. Körbel, C. Elsässer, H. Kungl, J. Acker, M.J. Hoffmann, Interactions of defect complexes and domain walls in CuO-doped ferroelectric $(K,Na)NbO_3$, Applied Physics Letters **102**, 242908 (2013).

[11] J. Hreščak, A. Bencan, T. Rojac, B. Malič, The influence of different niobium pentoxide precursors on the solid-state synthesis

of potassium sodium niobate, Journal of the European Ceramic Society **33**, 3065-3075 (2013).

[12] M.R. Bafandeha, R. Gharahkhani, J.-S. Lee, Comparison of sintering behavior and piezoelectric properties of (K,Na)NbO_3--based ceramics sintered in conventional and microwave furnace, Materials Chemistry and Physics **143**, 1289-1295 (2014).

[13] P. Bharathi, K.B.R. Varma, Effect of the Addition of B_2O_3 on the Density, Microstructure, Dielectric, Piezoelectric and Ferroelectric Properties of $K_{0.5}Na_{0.5}NbO_3$ Ceramics, Journal of Electronic Materials **43**, 2, 493-505 (2014).

[14] L.A. Ramajo, J. Taub, M.S. Castro, Effect of ZnO Addition on the Structure, Microstructure and Dielectric and Piezoelectric Properties of $K_{0.5}Na_{0.5}NbO_3$ Ceramics, Materials Research **17**, 3, 728-733 (2014).

[15] P. Bomlai, S. Sukprasert, S. Muensit, S.J. Milne, Phase development, densification and dielectric properties of (0.95-x) $Na_{0.5}K_{0.5}NbO_3$-0.05$LiTaO_3$-x$LiSbO_3$ lead free piezoelectric ceramics, Songklanakarin Journal of Science Education and Technology **30**, 6, 791-797 (2008).

[16] V.J. Tennery, K.W. Hang, Thermal and X-ray diffraction studies of $NaNbO_3$-NbO_3 system, Journal of Applied Physics **39**, 4749-4753 (1968).

[17] J. Rodel, W. Jo, K.T.P. Seifert, E.M. Anton, T. Graznow, D. Damjanovic, Perspective on the Development of Lead-free Piezoceramics, Journal of the American Ceramic Society **92**, 6 1153-1177 (2009).

[18] H.M. Rietveld, A profile refinement method for nuclear and magnetic structures, Journal of Applied Crystallography **2**, 65-71 (1969).

[19] M. Morawiec, A. Grajcar, Some aspects of the determination of retained austenite using the Rietveld refinement, Journal of Achievements in Materials and Manufacturing Engineering **80**, 1, 11-17 (2017).

[20] R. Rani, S. Sharma, Influence of sintering temperature on densification, structure and microstructure of Li and Sb Co-Modified (K,Na)NbO_3-based ceramics, Materials Sciences and Applications **2**, 1416-1420 (2011).

[21] S. Qian, K. Zhu, X. Pang, J. Wang, J. Liu, J. Qiu, Influence of sintering temperature on electrical properties of $(K_{0.4425}Na_{0.52}Li_{0.0375})(Nb_{0.8825}Sb_{0.07}Ta_{0.0475})O_3$ ceramics without phase transition induced by sintering temperature, Journal of Advanced Ceramics **2**, 4, 353-359 (2013).

[22] R.E. Jaeger, L. Egerton, Hot-pressing of potassium sodium niobates, Journal of the American Ceramic Society **45**, 5, 209-213 (1962).